

Structure of $\text{Ba}_2\text{In}_{2-x}\text{V}_x\text{O}_{5+x}$ phases: complementarity of diffraction, Raman and absorption techniques

A. Rolle, S. Daviero-Minaud, P. Roussel, A. Rubbens, R. N. Vannier

Equipe de Chimie du Solide – UCCS – Unité de Catalyse et Chimie du Solide – CNRS UMR
8181, USTL-ENSCL, BP 90 108, 59652 Villeneuve d'Ascq Cedex, France

Email: Aurelie.Rolle@ensc-lille.fr

Abstract

By combining X-ray and neutron diffraction with Raman and X-ray absorption spectroscopies, the location of vanadium in the structure of the $\text{Ba}_2\text{In}_{2-x}\text{V}_x\text{O}_{5+x}$ solid solution and its local environment was evidenced. Vanadium is spread over the two Indium sites of the Brownmillerite structure but its surrounding is tetrahedral. This involves the introduction of oxygen vacancies in the “octahedral” layers of $\text{Ba}_2\text{In}_2\text{O}_5$ and the presence of Indium with a VI fold coordination in the “tetrahedral” layers. The number of InO octahedra increases with the substitution rate which explains the stabilisation of cubic forms for substitution rate higher than 0.3.

Keywords: Brownmillerite, oxide ion conductor, barium oxide, indium oxide, $\text{Ba}_2\text{In}_2\text{O}_5$, neutron diffraction, X-ray diffraction, X-ray absorption spectroscopy, Raman scattering

1. Introduction

Because of its oxide ion conduction properties, $\text{Ba}_2\text{In}_2\text{O}_5$ has a potential of application as electrolyte for solid oxide fuel cells, oxygen generating systems or membrane for dense catalytic reactors [1-4]. At room temperature, it adopts the Brownmillerite structure. Its

hal-00187465, version 1 - 14 Nov 2007

symmetry is orthorhombic and it can be described as a defective perovskite composed of alternating “octahedral” ($\text{In}(1)\text{O}_6$) and “tetrahedral” ($\text{In}(2)\text{O}_4$) layers. It can also be viewed as an oxygen-ordered-vacancy defect perovskite in which one-sixth of the oxygen ions of the perovskite structure is replaced by an ordered array of vacancies. When the temperature increases, the symmetry becomes tetragonal ($T > 925^\circ\text{C}$) and then cubic ($T > 1040^\circ\text{C}$). These high temperature forms are highly oxide ion conductive [2,3,5-9]. With the aim to stabilize these two polymorphs at lower temperatures, numerous substitutions on the indium site, on the barium site or on both sites were reported in the literature. Our group considered the partial substitution for indium with vanadium, molybdenum and tungsten [10]. Solid solutions were evidenced for the three dopants. For vanadium compounds, $\text{Ba}_2\text{In}_{2-x}\text{V}_x\text{O}_{5+x}$, the solid solution limit was found in between $x=0.4$ and $x=0.5$. Its symmetry is orthorhombic for $0 \leq x < 0.2$, tetragonal for $x=0.2$ and cubic for $x \geq 0.3$. In the orthorhombic form, there are two possibilities of location for the dopant, in the octahedral or in the tetrahedral layers. Moreover, vanadium is known to easily adopt several coordinations, IV, V or VI and its actual surrounding is therefore not obvious. The determination of the dopant location in the vanadium solid solution and its local surrounding is the aim of this paper. In that frame, neutron diffraction, X-ray diffraction, Raman scattering and X-ray absorption spectroscopy were combined.

2. Experimental

The doped phases $\text{Ba}_2\text{In}_{2-x}\text{V}_x\text{O}_{5+x}$ with $x=0.1, 0.2, 0.3, 0.4$ were prepared as described in [10]. The compositions were checked by Energy Dispersive Spectroscopy and found to be in very good agreement with the starting compositions.

The structure of composition $x=0.1$ was refined by combining X-ray and neutron diffraction data. X-ray diffraction data were collected at room temperature on a Bruker axs D8

Advance diffractometer, equipped with a SolX energy dispersive detector, in the 5-100° range ($\lambda_{\text{CuK}\alpha}=1.5418 \text{ \AA}$) with a step of 0.02°. Neutron diffraction data were collected at room temperature on the high resolution powder diffractometer D2B at the Institut Laue Langevin (I.L.L.) at Grenoble. Approximately 20 g of compound were placed in a quartz tube open at one end and data were collected in the 0.3-130° range with a step of 0.05° at a wavelength of 1.594 Å. X-ray and neutron diffraction data were refined together using the beta version of JANA 2006 software, option powder [11]. The Rietveld method was applied.

Raman spectra were recorded at room temperature with the 647.1 nm excitation line from a Spectra Physics krypton ion laser. The beam was focused onto the sample using the macroscopic configuration of the apparatus. The scattered light was analyzed with an XY Raman Dilor spectrometer equipped with an optical multichannel charge coupled device liquid nitrogen –cooled detector. Acquisition and data processing were performed with the LABSPEC software.

X-ray absorption spectroscopy was performed at the Elettra Synchrotron in Trieste (Italy), on the BL 11.1 (XAFS) line with a Si (111) double monochromator, at the vanadium K edge (5465 eV) and at the indium L_I edge (4237 eV). Indeed, for this later, the energy range of the Elettra Synchrotron does not make possible to reach the K edge. The XANES data were collected at the Vanadium K edge on fluorescence mode and in transmission mode at the Indium L_I edge with a 0.2 eV step and an integrating time of 3 seconds per step near the edges, and 1 eV step further. In order to increase the signal quality, a minimum of 3 spectra were summed for each compound. For energy calibration, vanadium (energy range: 5450-5550 eV) and zinc (energy range: 9640-9690 eV) metal foils were used as references. The XANES spectra were normalized, after a linear subtraction of the pre-edge background absorption, to a value far enough from the absorption edge that coincides with a zero of the EXAFS signal.

3. Results and discussion

3.1. Dopant location in the Brownmillerite structure

The structure was refined by combining X-ray and neutron diffraction data. The structural model of the $\text{Ba}_2\text{In}_2\text{O}_5$ described in the $Icmm$ space group was used. In this model, In(2) and O(3) are located in a (8i) site with a partial occupancy of 0.5 which allows two possible orientations for the tetrahedra in the In(2)O layers as shown by TEM [12]. The wavelength of neutron being not accurate, it was refined with the unit cell parameters of this composition constrained to the value obtained from X-ray diffraction data. This led to a value of $\lambda = 1.5941(2)\text{\AA}$. The profiles were described by a pseudo-Voigt function and the backgrounds were determined manually. The result of the refinement is given in Table 1. The observed, calculated diffraction patterns and the corresponding differences are reported in Fig. 1 a and b. Vanadium was first introduced in both In(1) and In(2) sites with a constrain on their occupancy to verify the initial composition. Occupancies were refined in the last step of the refinement. A Fourier difference was calculated and revealed an extra oxygen position at $(\frac{1}{4}, \frac{1}{4}, \frac{1}{4})$. This extra oxygen site was then introduced in the refinement and occupancies of all oxygen sites were refined with constrain: the sum of their occupancies had to be equal to the expected oxygen stoichiometry. The thermal motions of all atoms were described using anisotropic parameters. The refinement revealed that vanadium substitutes both sites with occupancies of 0.044(4) and 0.056(4) in the In(1) (octahedral layers) and In(2) (tetrahedral layers) sites, respectively. Vacancies are also to be noticed in the O(1) and O(2) oxygen sites whereas the O(3) oxygen site is fully occupied. Interestingly, although these numbers must be taken with care because of the accuracy, the refinement led to the same amount of oxygen vacancy in the O(1) site (equatorial site of the octahedral InO layers), as vanadium in the In(1) site.

3.2. Local environment of metal in the structure

3.2.1. Raman spectroscopy

To define the local environment of vanadium in the structure, Raman scattering was performed on several compositions, $x=0$, $x=0.1$, $x=0.2$ and $x=0.3$. The spectra were compared to those of references carefully chosen for the different surrounding of vanadium and indium: $\text{Ba}_3(\text{VO}_4)_2$ in which the vanadium environment is composed of isolated tetrahedra, V_2O_5 whose structure is built upon square pyramids and In_2O_3 in which indium has an irregular octahedral environment. These spectra are given in Fig. 2. $\text{Ba}_3(\text{VO}_4)_2$ exhibits four bands at 837, 780, 380 and 328 cm^{-1} which are typical of tetrahedral VO_4 species [13]. These bands are also found in the substituted compounds at the same frequency values. However, they are broadened. The broadening increases with the substitution rate, it is characteristic of disorder. A tetrahedral surrounding for vanadium is confirmed by the bands observed in the $250 - 400\text{ cm}^{-1}$ frequency range which are assigned to angular deformations of the VO_4 entity. For an octahedral environment, bands at frequency above 900 cm^{-1} would be expected [14], which is not the case. The absence of lines around 996 cm^{-1} as observed for V_2O_5 excludes the possibility of square pyramids. These observations are therefore in agreement with a tetrahedral geometry for vanadium in different oxygen environments. One can also noticed a decrease in intensity of the most important band observed at 605 cm^{-1} for $\text{Ba}_2\text{In}_2\text{O}_5$. This band could be assigned to stretching motions of the tetrahedral InO_4 group since no such line is observed for In_2O_3 . However, the response of indium oxides is far lower than that of vanadium oxides and one can not conclude on the indium environment from Raman spectroscopy only.

3.2.2. XAFS spectroscopy

To confirm the local surrounding of the dopant and to characterise the evolution of the Indium environment according to the substitution rate, XAFS experiments were performed.

From these experiments, the oxidation number of these elements was also confirmed. A few X-ray absorption spectroscopy studies have already been reported on $\text{Ba}_2\text{In}_2\text{O}_5$ type compounds. Uchimoto *et al.* [15, 16] and Yao *et al.* [17] carried out EXAFS studies at the indium K edge on gallium and gadolinium doped compounds. The partial substitution of the barium site with lanthanum was also considered [18]. To our knowledge, no XAFS analysis on other doped compounds was reported in the literature. Here, the experiments were carried out at the vanadium K edge and at the indium L_1 edge to provide information on their local environment geometry and valence.

3.2.2.1. The vanadium K edge

Through the study of the characteristic pre-edge involved in the $1s \rightarrow 3d$ transition, XANES data can give qualitative information on the site symmetry. Indeed, this transition is forbidden in a regular octahedral symmetry, but becomes possible for irregular sites. The most intense pre-edge is then observed for tetrahedral symmetry.

Experiments were performed on $\text{Ba}_2\text{In}_{2-x}\text{V}_x\text{O}_{5+x}$ with $x=0.1$ (orthorhombic), $x=0.2$ (tetragonal), $x=0.3$ (cubic) and $x=0.4$ (cubic). Crystallised reference compounds were carefully selected according to their well characterized vanadium environment and valence: $\text{Ba}_3(\text{VO}_4)_2$ (V^{V}) in which the vanadium environment is composed of isolated tetrahedra and $\text{VO}_4(\text{V}^{\text{IV}})$ where the vanadium is in a distorted octahedral environment.

As shown in Fig. 3a, the spectra of the substituted compounds are almost the same. They are characterised by the existence of an intense pre-edge nearly as high as $\text{Ba}_3(\text{VO}_4)_2$ one and at the same energy. This confirms the Raman results. In the substituted compounds, the vanadium environment is therefore mainly tetrahedral, which is consistent with the presence of vacancies in the octahedral layer. Their edge position is similar to that of $\text{Ba}_3(\text{VO}_4)_2$, the valence of the vanadium in these compounds is then equal to V.

3.2.2.2. The indium L_I edge

The XAFS spectra at L_I edge were recorded on $Ba_2In_{2-x}V_xO_{5+x}$ compositions with $x=0.1$ (orthorhombic) and $x=0.3$ (cubic). The selected crystallised references were $Ba_2In_2O_5$ in which the indium atom has in octahedral and tetrahedral environment and In_2O_3 where it has an irregular octahedral environment. The XANES signal obtained at the indium L_I edge for doped compounds is similar to $Ba_2In_2O_5$ one (Fig. 3b): the indium atom has a mixed octahedral-tetrahedral environment. However, the intensity of the edge increases with the substitution rate and becomes closer to In_2O_3 one which supports an increase of octahedral environment for indium when the substitution rate increases.

Whatever the substitution rate, the indium atom has a more octahedral medium environment than in the undoped $Ba_2In_2O_5$. This is in good agreement with the tetrahedral environment of the vanadium described previously. Indeed as the vanadium environment is tetrahedral, the number of indium atoms having an octahedral environment has to increase, all the more than the partial substitution with vanadium implies the introduction of additional oxide ions.

4. Conclusions

By combining X-ray and neutron diffraction with Raman and X-ray absorption spectroscopies, the location of vanadium in the structure of the $Ba_2In_{2-x}V_xO_{5+x}$ solid solution and its local environment was evidenced. Vanadium is spread over the two Indium sites of the Brownmillerite structure but its surrounding is tetrahedral. This involves the introduction of oxygen vacancies in the “octahedral” layers of $Ba_2In_2O_5$ and the presence of Indium with a VI fold coordination in the “tetrahedral” layers. The number of InO octahedra increases with the substitution rate which explains the stabilisation of cubic forms for substitution rate higher than 0.3.

Acknowledgements

The Institut Laue Langevin is thanked for providing neutron facilities and Dr. Emmanuelle Suard (Institut Laue Langevin) is gratefully acknowledged for helpful discussions. Dr Belin (local contact on an EXAFS line – ex Lure, Soleil, France) and Dr Olivi (local contact on an EXAFS line – Elettra, Trieste, Italy) are acknowledged for their help and availability. The authors are very grateful to L. Burylo for X-ray diffraction. The « Fonds Européen de Développement Régional (FEDER) », the « Centre National de la Recherche Scientifique » (CNRS), the « Région Nord Pas-de-Calais » and the « Ministère de l'Education Nationale, de l'Enseignement Supérieur et de la Recherche » are acknowledged for fundings of X-ray diffractometers. A. R. is grateful to the CNRS and the « Région Nord Pas-de-Calais » for the funding of her PhD grant. V. Petricek is acknowledged for providing us the JANA 2006 beta Version allowing the combined refinement of X-ray and neutron data

References

- [1] D. H. Gregory, M. T. Weller, J. Solid State Chem. 107 (1) (1993) 134.
- [2] S. B. Adler, J. A. Reimer, J. Baltisberger, U. Werner, J. Am. Chem. Soc. 116 (1994) 675.
- [3] S. A. Speakman, J. W. Richardson, B. J. Mitchell, S. T. Misture, Solid State Ionics 149 (2002) 247.
- [4] J.B. Goodenough, J.E. Ruiz-Diaz, Y.S Zhen, Solid State Ionics 44 (1990) 21.
- [5] T. R. S. Prasanna, A. Navrotsky, J. Mater. Res. 8 (1993) 1484.
- [6] G. B. Zhang, D. M. Smyth, Solid State Ionics 82 (1995) 161.
- [7] M. Kanzaki, A. Yamaji, Mater. Sci. and Eng. B41 (1996) 46.
- [8] T. Hashimoto, Y. Ueda, M. Yoshinaga, K. Komazaki, K. Asaoka and S. Wang, J. Electrochem. Soc. 149 (2002) 1381.

- [9] T. Hashimoto, K. Asaoka, K. Komazaki, Y. Ueda, M. Yoshinaga, *Electrochemical Society Proceedings* 28 (2001) 291.
- [10] A. Rolle, R. N. Vannier, N. V. Giridharan, F. Abraham, *Solid State Ionics* 176 (2005) 2095.
- [11] V. Petricek, M. Dusek, L. Palatinus, *The crystallographic computing system JANA 2006 beta version*, Institute of Physics, Praha, Czech Republic, 2007.
- [12] P. Berastegui, S. Hull, F.J. Garcia-Garcia, S.G. Erikson, *J. Solid State Chem.* 164 (2002) 119.
- [13] A. Lorriaux-Rubbens, J. Corset, J. Ghamri, H. Baussart, *Ad. Mater. Research*, Vols 1-2 (1994) 433.
- [14] R.L. Frost, K.L. Erickson, M.L. Weier, O. Carmody, *Spectrochim. Acta*, A61 (2005) 829.
- [15] Y. Uchimoto, M. Kinuhate, T. Yao, *Japanese Journal of Applied Physics* 38 (1998) 111, International Conference Synchrotron Radiation in Materials Science SRMS-2, Kobe, Japan.
- [16] Y. Uchimoto, M. Kinuhata, H. Takagi, T. Yao, T. Inagaki, H. Yoshida, *Electrochemical Society* 19 (1999) 317.
- [17] T. Yao, Y. Uchimoto, M. Kinuhata, T. Inagaki, H. Yoshida, *Solid State Ionics* 132 (2000) 189.
- [18] Y. Uchimoto, H. Takagi, T. Yao, N. Ozawa, T. Inagaki, H. Yashida, *Journal of Synchrotron Radiation* 8 (2001) 857.

Table captions

Table 1. Structural model described in the space group $Icmm$ deduced from the combined refinement of neutron diffraction and X-ray diffraction data corresponding to $Ba_2In_{2-x}V_xO_x$ with $x=0.1$ at room temperature.

Tables

Table 1. Structural model described in the space group $Icmm$ deduced from the combined refinement of neutron diffraction and X-ray diffraction data corresponding to $Ba_2In_{2-x}V_xO_x$ with $x=0.1$ at room temperature.

a (Å)	b (Å)	c (Å)	volume (Å ³)	density
6.0564 (3)	16.8085 (9)	5.9698 (3)	607.72 (8)	6.33 (6)

atom	site	x	y	z	occupancy	U_{eq}^* (Å ²)
Ba	8(h)	0.5081(4)	0.61103(9)	0	1	0.0101(8)
In(1)	4(a)	0	0	0	0.956(4)	0.011(1)
V(1)	4(a)	0	0	0	0.044(4)	0.011(1)
In(2)	8(i)	0.5519(4)	0.25	0.5	0.944(4)	0.011(1)
V(2)	8(i)	0.5519(4)	0.25	0.5	0.056(4)	0.011(1)
O(1)	8(g)	0.25	0.9942(2)	0.25	0.978(4)	0.0132(9)
O(2)	8(h)	0.0466(6)	0.1379(2)	0	0.986(6)	0.029(1)
O(3)	8(i)	0.6374(4)	0.25	0.1382(1)	0.5	0.038(3)
O(4)	4(c)	0.25	0.25	0.25	0.17(2)	0.038(3)

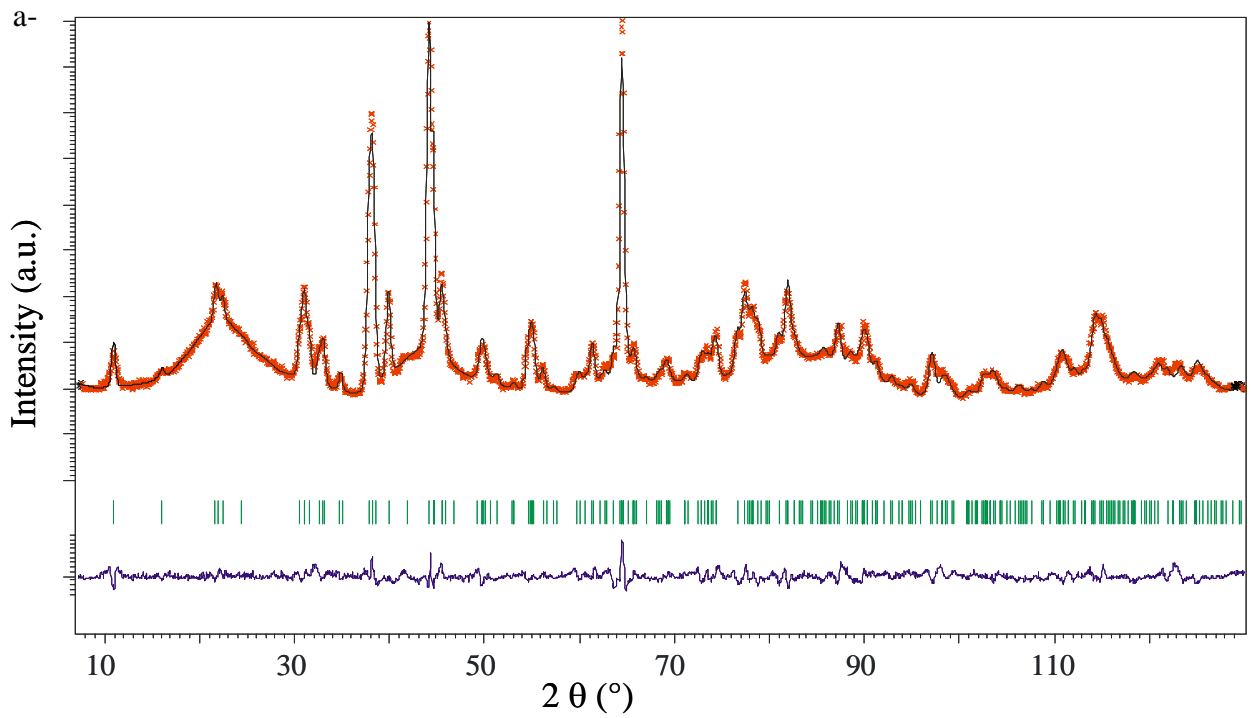
*	U_{11}	U_{22}	U_{33}	U_{12}	U_{13}	U_{23}
Ba	0.020(2)	0.01(1)	0.001(1)	0.002(2)	0	0
In(1)	0.012(2)	0.012(2)	0.008(2)	0.004(2)	0	0
V(1)	0.012(2)	0.012(2)	0.008(2)	0.004(2)	0	0
In(2)	0.012(2)	0.012(2)	0.008(2)	0.004(2)	0	0
V(2)	0.012(2)	0.124(2)	0.008(2)	0.004(2)	0	0
O(1)	0.024(2)	0.013(2)	0.003(1)	0	0.003(1)	0
O(2)	0.047(3)	0.018(1)	0.021(2)	0.011(2)	0	0
O(3)	0.041(5)	0.031(4)	0.040(5)	0	0.008(3)	0
O(4)	0.041(5)	0.031(4)	0.040(5)	0	0.008(3)	0

Figure Captions

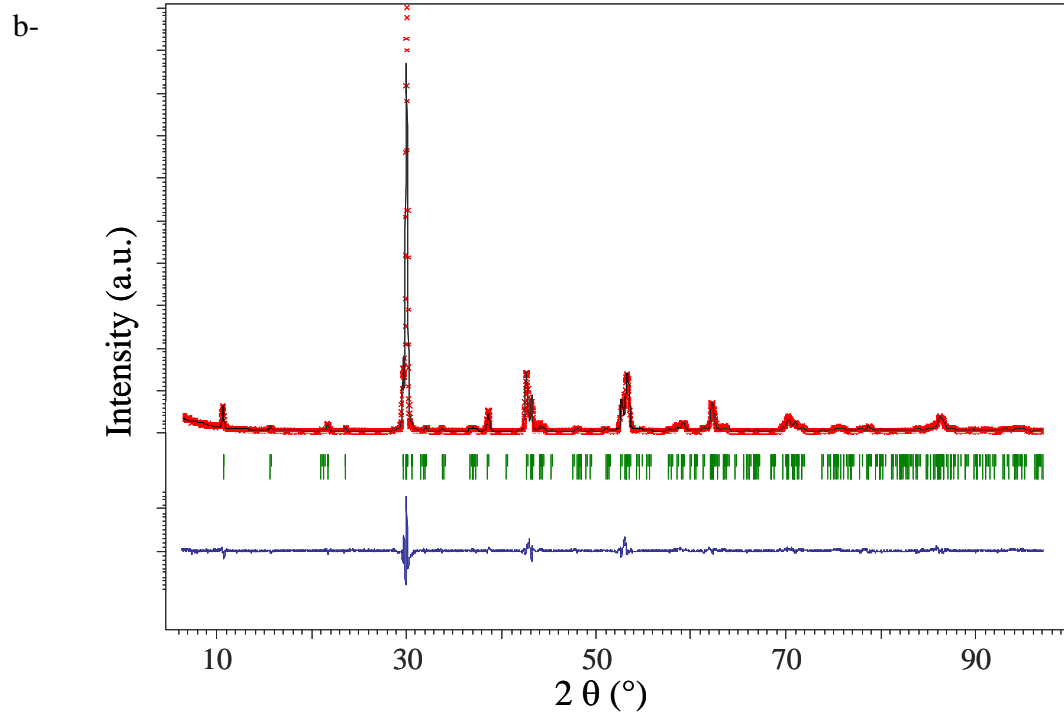
Fig. 1: a- Neutron diffraction pattern data and b- X-ray diffraction pattern, corresponding to $\text{Ba}_2\text{In}_{2-x}\text{V}_x\text{O}_{5+3x/2}$ with $x=0.1$, collected at room temperature

Fig. 2: Raman spectra of $\text{Ba}_2\text{In}_2\text{O}_5$ (a), In_2O_3 (b), $\text{Ba}_2\text{In}_{2-x}\text{V}_x\text{O}_{5+x}$: $x = 0.1$ (c), $x = 0.2$ (d), $x = 0.3$ (e), $\text{Ba}_3(\text{VO}_4)_2$ (f) and V_2O_5 (g).

Fig.3: a- XANES spectra at K edge of $\text{Ba}_2\text{In}_{2-x}\text{V}_x\text{O}_{5+x}$ with $x=0.1$ (orthorhombic), $x=0.4$ (cubic) compared to $\text{Ba}_3(\text{VO}_4)_2$ and VOSO_4 which are characterised by isolated tetrahedra and distorted octahedra, respectively, b- XANES spectra at L_{II} edge $\text{Ba}_2\text{In}_{2-x}\text{V}_x\text{O}_{5+x}$ compounds with $x=0.1$ (orthorhombic), $x=0.4$ (cubic) compared to In_2O_3 and $\text{Ba}_2\text{In}_2\text{O}_5$ references, in which the indium has respectively an irregular environment and a mixed octahedral-tetrahedral environment.



R_{obs}	R_{wobs}	R_{all}	R_{wall}	R_p	R_{wp}
3.56	2.90	3.57	2.90	2.44	3.13



R_{obs}	R_{wobs}	R_{all}	R_{wall}	R_p	R_{wp}
6.49	4.61	6.84	4.62	12.81	16.67

Fig. 1.

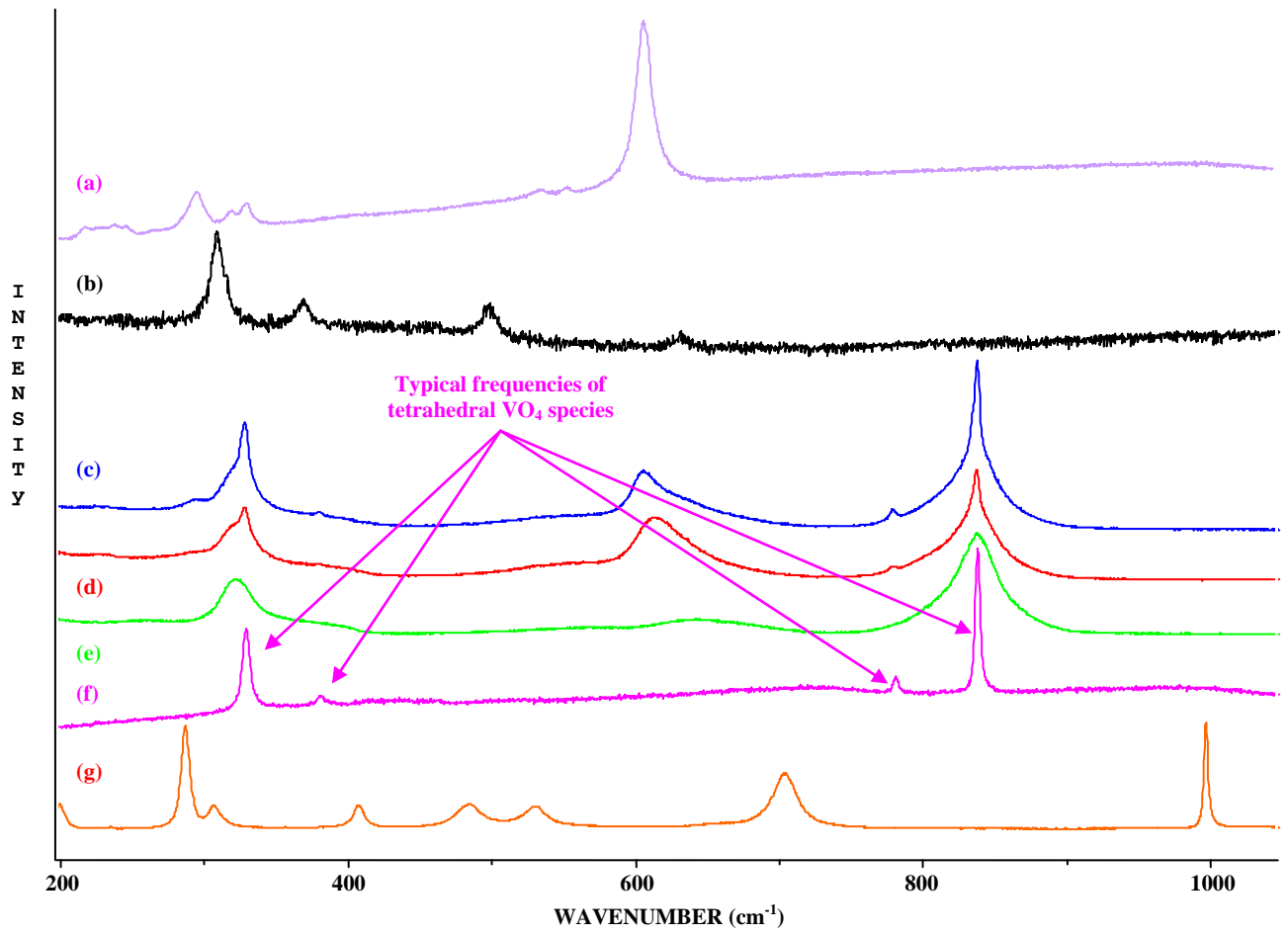


Fig. 2.

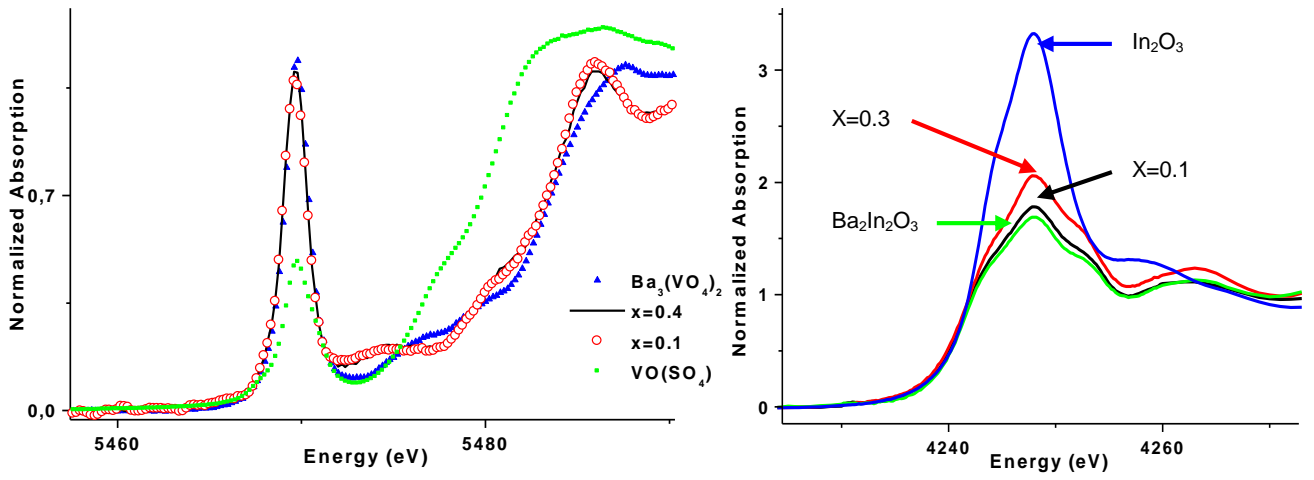


Fig.3.